

Local order and XAFS spectra of metal-metalloid glasses

This article has been downloaded from IOPscience. Please scroll down to see the full text article.

1991 J. Phys.: Condens. Matter 3 5153

(<http://iopscience.iop.org/0953-8984/3/27/008>)

View [the table of contents for this issue](#), or go to the [journal homepage](#) for more

Download details:

IP Address: 171.66.16.147

The article was downloaded on 11/05/2010 at 12:19

Please note that [terms and conditions apply](#).

Local order and XAFS spectra of metal–metaloid glasses

A M Bratkovsky†§ and A V Smirnov‡

† IRC in Superconductivity, University of Cambridge, Downing Street, Cambridge CB2 3EQ, UK

‡ IV Kurchatov Institute for Atomic Energy, 123182 Moscow, USSR

Received 13 September 1990, in final form 19 February 1991

Abstract. The study of local order in Ni–B and Fe–B model glasses by the Monte Carlo simulation method is presented. Despite the simple model for inter-atomic interaction used, the calculated radial distribution functions and generalized Warren chemical short-range order parameters are in quite reasonable agreement with high-resolution neutron diffraction data. Analysis of the bond-angle distribution indicates the existence of icosahedral motifs in the metal subsystem and the appearance of direct B–B contact in $\text{Ni}_{66}\text{B}_{34}$ glass with coordination number $Z_{\text{BB}} = 0.75$ (the experimental value is $Z_{\text{BB}} = 0.9 \pm 0.1$). The local order in glasses with ratio of components transition metal–metal (TM: M) equal to 80:20 and 66:34 changes noticeably under amorphisation and results in changes in x-ray absorption fine structure (XAFS) spectra. XAFS spectra appear to be sensitive to the local symmetry at the absorbing site and to higher-order coordination shells, especially around the metalloid atom. The calculated XAFS spectra may be used together with precise measurements to verify the structural models and provide information about the higher-order correlations.

1. Introduction

The origin of the local atomic order in metallic glasses and its inter-connection with other physical properties, such as mechanical and magnetic properties etc, remains an open problem. The problem of stability and relaxation in glasses seems to be one of the most intriguing. Some recent theories indicate the relevance of stability of simple glasses to possible icosahedral ordering in the glassy state [1]. For the most important case of multi-component systems this correlation is not clear and should be investigated. It is supported by the recent computer simulation of the well-known Lennard–Jones glass [2]. In this problem we can, of course, go beyond the study of radial distribution functions (RDF), which are now well known from high-resolution x-ray and neutron diffraction experiments with isotopic substitution techniques. In the present paper we will concentrate on studying the two-component glasses Fe–B and Ni–B, which have been widely treated theoretically and experimentally [3–7].

Local trigonal prismatic order was widely discussed as being relevant to the local coordination in metal–metaloid glasses. Here Ni–B glass is of special interest because it quenches into the amorphous state from a melt over a wide composition range (from 18 to 40 at. %B) and covers the crystalline (c) counterparts c- Ni_3B , c- Ni_2B and c- Ni_4B_3 .

§ On leave from IV Kurchatov Institute for Atomic Energy, 123182 Moscow, USSR.

Trigonal prismatic coordination of 6 TM atoms around a B atom is evident in $c\text{-TM}_3\text{B}$ (TM = Ni, Fe) and $c\text{-Ni}_4\text{B}_3$, but the local order in $c\text{-Ni}_2\text{B}$ is quite different from those mentioned above and consists of 8 Ni atoms forming an Archimedean antiprism [3, 4].

The analysis of experimental data [7] shows that coordination number Z_{BNi} decreases in Ni_2B under amorphization but the final value remains a subject of discussion. It should be mentioned here that the results from high-resolution neutron-diffraction studies [4, 5] indicate a reduction of Z_{BNi} to 5.2–5.8 in $\text{Ni}_{1-x}\text{B}_x$ in the wide range 18–40 at.%B, and the appearance of direct B–B contact (forbidden in the Polk and other models [27, 3]) becomes evident with $Z_{\text{BB}} = 0.9 \pm 0.1$ [5]. We anticipate that the local boron environment will change drastically under amorphization of $c\text{-Ni}_2\text{B}$, and try to find some manifestation of it.

To go beyond the pair correlations we can analyse the bond-angle distribution [6, 7], calculating rotational invariants of second and third order (Q_1 and W_1 , respectively), introduced by Steinhardt *et al* [8], or analogous characteristics. To find the tendency towards an icosahedral type of local order we have to compare the bond-angle distribution with that for the system with exact five-fold symmetry. Therefore, we can compare the results with bond-angle distribution in a 3D Penrose tiling rather than with that for a single icosahedron [2], by which it is impossible to fill the whole space without voids. The results can be partially verified by a bond-angle sensitive technique, such as the measurements of x-ray absorption fine structure (XAFS) [9–11] in comparison with their crystalline counterparts.

Below we shall discuss the Monte Carlo model of the atomic structure of Fe–B and Ni–B glasses, especially the interesting amorphous (a-) system $a\text{-Ni}_{66}\text{B}_{34}$, in comparison with its crystal counterpart.

2. Atomic structure

To study higher-order correlations in the amorphous state we must have the model describing at least the radial distribution function (RDF) reasonably well. The most convenient method is to start from a model of inter-atomic interactions and then to construct the atomic model by means of a computer simulation [12, 13]. Despite the possible covalent effects due to strong hybridization of TM 3d-electrons with M 2p-electrons [6, 14] the realistic choice of a simplest model of pairwise inter-atomic potentials is possible, providing a reasonable description of RDFs, coordination numbers and density [12, 15]. The correlation of calculated properties with available experimental data is a crucial test of the validity of the model. Small effects of covalent bonding on the structural properties of TM–M glasses perhaps reflects the relative weakness of M–M interactions [15].

The outstanding progress in parameter-free simulations of structural and electronic properties of sp-bonded systems was achieved in recent years within the Car–Parrinello method [16, 17]. In this method the ionic and electronic degrees of freedom are treated equally, using the electron density functional method combined with molecular dynamics, a simulated annealing technique and a pseudopotential description of electron–ion interactions. Regrettably, this method is not directly applicable for the systems under consideration, because the behaviour of the highly localized TM d-electrons is hardly tractable within the plane-wave basic functions used in a pseudopotential scheme.

To prepare the liquid and glassy states we have used the classical Monte Carlo method [6, 7] with the Morse-type central potential for inter-atomic interaction between α - and β -type species [12, 18]

$$\varphi_{\alpha\beta}(r) = \varepsilon_{\alpha\beta} \{ \exp[-2\gamma(r/\sigma^{\alpha\beta} - 1)] - 2\exp[-\gamma(r/\sigma^{\alpha\beta} - 1)] \} f(r/\sigma^{\alpha\beta}), \quad (1)$$

$$f(x) = \begin{cases} 1 & x < 1 \\ 3z^4 - 8z^3 + 6z^2 & 1 < x < r_c^{\alpha\beta}/\sigma^{\alpha\beta} \\ 0 & x > r_c^{\alpha\beta}/\sigma^{\alpha\beta} \end{cases}$$

where $z = (x - r_c^{\alpha\beta}/\sigma^{\alpha\beta}) / (1 - r_c^{\alpha\beta}/\sigma^{\alpha\beta})$, $\gamma = 3.76$, $r_c^{\alpha\beta}/\sigma^{\alpha\beta} = 1.4$, $\varepsilon_{\text{FeFe}} = \varepsilon_{\text{NiNi}} = 0.52$ eV, $\varepsilon_{\text{FeB}} = \varepsilon_{\text{NiB}} = 1.07\varepsilon_{\text{FeFe}}$, $\varepsilon_{\text{BB}} = 0.047\varepsilon_{\text{FeFe}}$, $\sigma_{\text{FeFe}} = 2.585$ Å, $\sigma_{\text{NiNi}} = 2.532$ Å, $\sigma_{\text{FeB}} = 2.056$ Å, $\sigma_{\text{NiB}} = 2.015$ Å, $\sigma_{\text{BB}} = 3.36$ Å (for Fe-B), $\sigma_{\text{BB}} = 2.28$ Å (for Ni-B). The choice of parameters of inter-atomic potentials (1), is not strictly justified but it reproduces the experimental data [5] rather well (see discussion in [7, 15] and below). We have studied the systems containing 500 atoms in a cubic box with periodic boundary conditions.

To analyse the local order we have calculated the total and partial RDF $g_{\alpha\beta}(r)$ and reduced RDF

$$G_{\alpha\beta}(r) = 4\pi nr(g_{\alpha\beta}(r) - 1) \quad (2)$$

where n is the density.

To study the bond-angle distribution, we have calculated the bond orientational parameters of Steinhardt *et al* [8], generalized in [6] and [7] for the case of multi-component systems. The rotational invariants are constructed from the set of partial bond-order parameters

$$Q_{lm}^{\alpha\beta} = \langle Y_{lm}(r_{\alpha\beta}) \rangle. \quad (3)$$

Here $r_{\alpha\beta}$ is a bond vector and $\langle \dots \rangle$ denotes the averaging over bonds connecting the given atom of type α and its nearest neighbours of type β ; $Y_{lm}(r_{\alpha\beta})$ are the usual spherical harmonics. The nearest neighbours were defined by the Voronoi tessellation and a search of the atoms sharing the common face of the given polyhedron. We can then construct the invariants of second and third order.

$$Q_l^{\alpha\beta} = \left(\frac{4\pi}{2l+1} \sum_{m=-l}^l |Q_{lm}^{\alpha\beta}|^2 \right)^{1/2} \quad (4)$$

$$W_l^{\alpha\beta} = \sum_{m_1+m_2+m_3=0} \begin{pmatrix} l & l & l \\ m_1 & m_2 & m_3 \end{pmatrix} Q_{lm_1}^{\alpha\beta} Q_{lm_2}^{\alpha\beta} Q_{lm_3}^{\alpha\beta} \quad (5)$$

where we used the known Wigner 3j-symbols.

When we are interested in bond angle distribution only it seems to be more useful to analyse the parameters p_l defined as follows

$$p_l = \langle \mathcal{P}_l \rangle \quad (6a)$$

$$\mathcal{P}_l = (N_b Q_l^2 - 1) / (N_b - 1) / (N_b - 1) = \frac{1}{N_b(N_b - 1)} \sum_{i,j=1, i \neq j}^{N_b} P_l(\cos \theta_{ij}) \quad (6b)$$

where θ_{ij} is an angle between bonds, connecting the atom at the origin with atoms i and

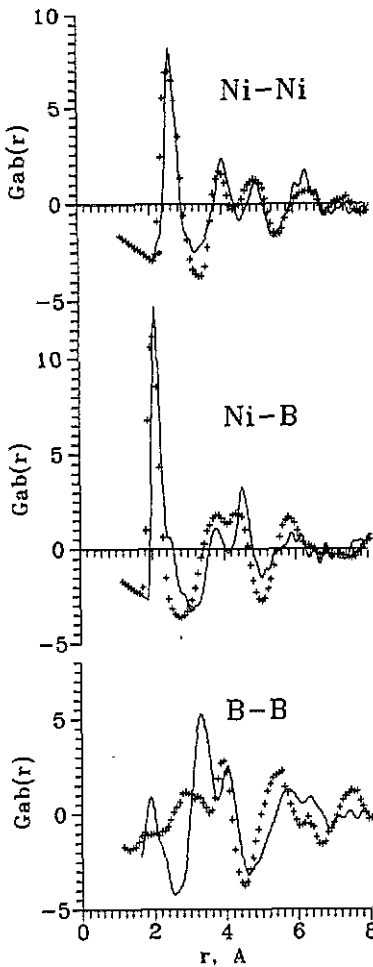


Figure 1. The reduced partial radial distribution functions $G(r)$ for $\text{Ni}_{66}\text{B}_{34}$ glass: experimental data [5] (full curve) and present work (crosses).

j , and N_b is the number of bonds connecting the atom at the origin with the nearest neighbours.

Glassy states of Fe-B and Ni-B systems were obtained via isochoric rapid quenching of the corresponding liquids. The calculated partial RDF has the usual peculiarities of glassy metals, except for B-B coordination in $\text{Ni}_{66}\text{B}_{34}$ (figure 1). This shows the narrow, high first peak and split second peak that reflects the non-trivial ordering on distances from 3 Å to 4.5 Å. The RDF of the boron atom in $\text{Ni}_{66}\text{B}_{34}$ shows the direct B-B contact in the amorphous phase with the first maximum at 1.7 Å (it becomes evident when we analyse the usual RDF $g(r)$ [7]). The calculated B-B correlations are, of course, only in qualitative agreement with experiment at low distances, below 4 Å, as a result of a less accurate choice of M-M interactions in the present model. The estimate of the B-B coordination number gives the value $Z_{\text{BB}} = 0.75$. This peculiar structure presumably arises from the interference of B-B and Ni-Ni pairs in the range 2 Å–2.5 Å although the B-B potential is predominantly a repulsive one with the first zero near 1.86 Å. Hence, the direct B-B contact found by experiment [5] and in our simulation of glassy $\text{Ni}_{66}\text{B}_{34}$ may be called the ‘packing frustration’ which means that it is impossible for Ni and B

Table 1. Generalized Warren short-range order parameters α_w and η_{BNi}^0 , as defined by (8–10) for a-Ni₆₆B₃₄. Experimental data are taken from [55].

	Theory	Expt.
α_w	-0.063	-0.076
$\alpha_w/\alpha_w^{\text{max}}$	0.12	0.15
η_{BNi}^0	0.56	0.46

atoms to occupy the same coordination shell around the B atom. This observation undermines the statement about the absence of direct M–M contact in TM_{1-x}M_x glasses up to $x = 33$ at. %M (see the discussion in [3, 15]).

The study of a generalized Warren [19] chemical short-range order (SRO) parameter, α_w , provides more information about the quality of the structural model. Following [13] we can find the concentration–concentration coordination number for Ni_{1-x}B_x:

$$Z_{\text{cc}} = c_{\text{B}}(Z_{\text{NiNi}} - Z_{\text{BNi}}) + c_{\text{Ni}}(Z_{\text{BB}} - Z_{\text{NiB}}) \quad (7)$$

where $c_{\text{B}} = x$ and $c_{\text{Ni}} = 1 - x$. Then we define the Warren parameter

$$\alpha_w = Z_{\text{cc}}/Z_w \quad \text{where } Z_w = c_{\text{B}}Z_{\text{Ni}} + c_{\text{Ni}}Z_{\text{B}}. \quad (8)$$

We note here that the condition $\alpha_w = 0$ indicates complete randomness and positive or negative values for α_w correspond to a preference for self-coordination or hetero-coordination, respectively. The maximum ordering is achieved when α_w has the maximum possible value

$$\alpha_w^{\text{max}} = -\min(c_{\text{B}}, c_{\text{Ni}})/\max(c_{\text{B}}, c_{\text{Ni}}). \quad (9)$$

We can also analyse the ‘unlike-atom chemical SRO coefficient’ [20]

$$\eta_{\text{BNi}}^0 = (Z_{\text{BNi}}\langle Z \rangle / c_{\text{Ni}}Z_{\text{B}}Z_{\text{Ni}} - 1) / \eta_{\text{BNi}}^{\text{max}} \quad (10)$$

where $\langle Z \rangle = c_{\text{Ni}}Z_{\text{Ni}} + c_{\text{B}}Z_{\text{B}}$ and

$$\eta_{\text{BNi}}^{\text{max}} = \min(c_{\text{Ni}}Z_{\text{Ni}}, c_{\text{B}}Z_{\text{B}}) / \max(c_{\text{Ni}}Z_{\text{Ni}}, c_{\text{B}}Z_{\text{B}}). \quad (11)$$

The value $\eta_{\text{BNi}}^0 = 0$ corresponds to a complete chemical disorder, positive and negative values indicate a preference for hetero-coordination and self-coordination, respectively. The actual values of SRO parameters, quoted in table 1, show a reasonable agreement between calculated and experimental data. Absolute values of SRO parameters are slightly overestimated in the present model, as in [13], but the difference does not exceed 20%. It again confirms that the pair correlations are adequately described by the present model.

A set of bond orientational parameters (6) was calculated for the glassy metals Fe–B and Ni–B and analysed in table 2 in comparison with a single icosahedron (ICOS), a 3D periodic Penrose lattice (PPL) [6], FCC and amorphous Lennard-Jones crystals (FCC-LJ, a-LJ) and in crystalline Ni₂B and Fe₃B. The distribution of $\langle p_l \rangle$ values ($l = 2, \dots, 10$) for *metal–metal* correlations are given for the glassy Ni–B and Fe–B together with the corresponding values for binary crystalline and monatomic systems. A set of p_l 's is useful for the analysis of changes in SRO atomic correlations, particularly for finding the probable five-fold atomic ordering [1, 2, 6, 7]. In [2], Steinhardt's parameters with $l = 6$, which have a remarkably high value for a single icosahedron in comparison with

Table 2. The bond orientational parameters p_l and the number of nearest neighbours N_b for a Lennard-Jones crystal (FCC-LJ) and glass (a-LJ), a single icosahedron (ICOS), a 3D periodic Penrose lattice (PPL) and for a metal-metal subsystem in crystalline Ni_2B (c- Ni_2B), Fe_3B (c- Fe_3B) and amorphous $\text{Ni}_{66}\text{B}_{34}$, $\text{Fe}_{30}\text{B}_{20}$ (a- NiB and a- FeB).

1	$p_l \times 10^2$					N_b
	2	4	6	8	10	
FCC-LJ	-7.2	-6.8	13.5	12.7	-6.5	14.0
c- Ni_2B	-8.3	-8.6	7.4	-5.1	-7.3	11
c- Fe_3B	-6.9	-2.5	2.4	1.0	5.0	12
a-LJ	-7.2	-7.0	7.9	1.2	-3.6	14.1
a- NiB	-6.9	-6.5	2.8	0.0	-1.7	14.2
a- FeB	-6.5	-5.9	5.7	0.9	-0.9	14.7
ICOS	-9.1	-9.1	38.9	-9.1	5.3	12
PPL	-7.4	-6.5	3.0	-6.1	-1.4	13.4

those in cubic lattices [8], were used for this purpose. However the criterion of a high W_6 value (or high p_6 , see table 2) is hardly applicable, since we need to deform the icosahedra when filling the whole space [7]; therefore, we must investigate the p_l distribution in any given system in comparison with the 3D Penrose lattice, which has an exact fivefold local coordination.

The results in table 2 indicate the deformation of the p_l -distribution under amorphization, especially for $l = 6, 8, 10$. The character of the deformation may be attributed to the coexistence of fivefold and FCC motifs in the local order of the Lennard-Jones glass. The FCC-like local coordination became less prominent in the Fe-B and Ni-B glasses and icosahedral motifs appeared in metal-metal correlations [7].

3. XAFS spectra

To calculate the probability of x-ray absorption we can firstly construct a crystal potential. We have used the LMTO method [21] to calculate the electronic structure of c- Ni_2B within the parameter-free electron density functional theory in the muffin-tin (MT) approximation [6]. Needless to say, the MT approximation is not good enough when implemented in the open structure, as in our case. Therefore, to achieve a correct value of the lattice constants (or zero total pressure) we have included two empty spheres into the boron plane to simulate the non-MT corrections to the electronic structure. The interesting feature of calculated electron density of states (DOS) is that the Fermi energy lies in the region of a local maximum in the DOS, formed by Ni 3d-electrons hybridized with B 2p-electrons. We anticipate that this picture, in general, persists in the amorphous phase too [14]. The self-consistent potentials computed in this way for both Ni and B were used in the calculation of XAFS spectra for c- Ni_2B and a- $\text{Ni}_{66}\text{B}_{34}$. The changes in the electron potentials in correspondence with changes in the atomic coordination under amorphization were ignored at this stage. In the MT approximation for the shape of the electron potential, the golden rule expression for the XAFS transition rate $W_c(\omega)$ factorizes on the imaginary part of the lattice Green function $g(r, r'; E)$ and the squared dipole matrix element for the core-band transition m_{cL} . Afterwards, $\text{Im } g(r, r'; E)$ is

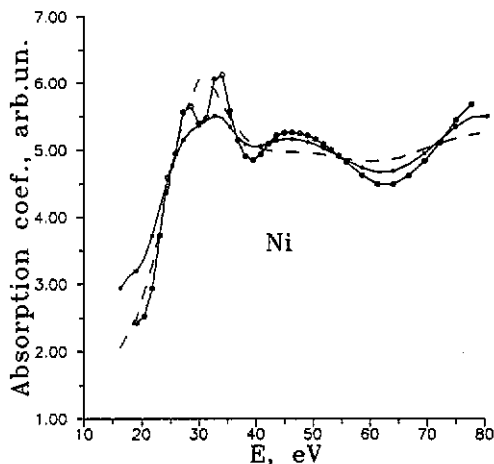


Figure 2. The Ni K-edge transition rate for c-Ni₂B and a-Ni₆₆B₃₄ (—○—○—○; crystal, $\Gamma = -0.02$ au; -*-*-: crystal, $\Gamma = -0.10$ au; ---: glass, $\Gamma = -0.02$ au).

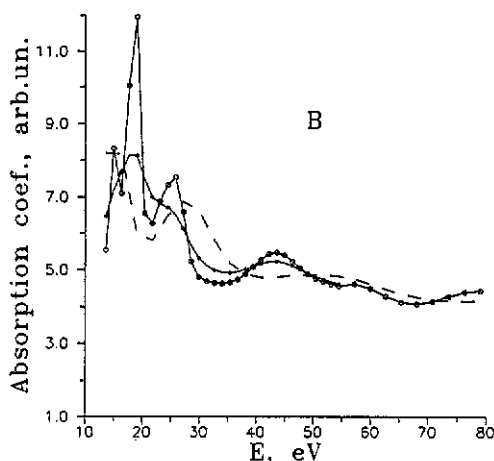


Figure 3. The B K-edge transition rate for c-Ni₂B and a-Ni₆₆B₃₄ (—○—○—○; crystal, $\Gamma = -0.02$ au; -*-*-: crystal, $\Gamma = -0.10$ au; ---: glass, $\Gamma = -0.02$ au).

calculated through the scattering path operator, τ_{LL}^{00} , which defines the probability for a photoelectron to return to the excited atom [22–24]. Because this quantity depends on the transparency of the neighbouring atomic shells it may be expressed through the reflection matrix of components R^{Of} as

$$\tau^{00} = [(t^0)^{-1} - R^{Of}]^{-1} \quad (12)$$

where t^0 is an atomic scattering amplitude. In the reflection matrix the single-back-scattering and more complex processes are treated equally [22–24]. Because the single-scattering processes dominate at higher energies, we can expand the formula for the transition rate and obtain [25]

$$W_c(\omega) = W_c^a(\omega) \left(1 + \sum_{n>1} \chi^n(k) \right) \quad (13)$$

where $W_c^a(\omega)$ is the atomic transition rate and

$$\chi^n(k) = \sum_i A^n(k, p_i) \sin(kR(p_i) + \varphi^n(k, p_i)) \quad (14)$$

is a partial contribution from the path p_i where a photoelectron scatters $n - 1$ times on the neighbouring atoms, $R(p_i)$ is a path length. The contribution of the scattering paths can be estimated from the expansion of the τ^{00} -matrix since $\tau^{00} = t + tgt + tgtgt + \dots$, where g is a known single-site atomic Green function.

The results of calculations of $W_c(\omega)$ within the exact matrix inversion (12) for c-Ni₂B and a-Ni₆₆B₃₄ are displayed in figures 2 and 3. In c-Ni₂B we have the enhanced transition rate in the region of first maximum, which is evidently formed by back-scattering on the first 8 Ni and 3 B neighbours placed at a distances of 2.14 Å and 2.12 Å, respectively. The nature of the low-energy prepeak (noticeable at the electron width $\Gamma = -0.02$ au) is not clear and may characterize the convergence of intermediate sums over the orbital quantum number (it also may be valid for the Ni K-edge absorption). The second peak

in the B K-edge absorption (near 25 eV) may correspond to the scattering on the second and third Ni shells containing 16 atoms, and to more complex trajectories as well. At a large electron width ($\Gamma = -0.10$ au) the second peak is smoother and becomes a hump. The behaviour of $W(\omega)$ become regular at $E > 40$ eV. In a-Ni₆₆B₃₄ the first peak shifts to a lower energy and the second peak shifts to a higher energy in correspondence with large changes in B–B and B–Ni local correlations under amorphization.

The picture described above is in close correspondence with the calculations of XAFS spectra for amorphous and crystalline Pd₈₀Ge₂₀ of the Ge K-edge [10]. In the latter case the splitting of first peak was attributed to the scattering processes in the second and third shells of the Ge environment. In both cases the changes in the next-nearest neighbour geometry result in significant change in x-ray absorption.

The Ni atom in c-Ni₂B is not as well-coordinated as the B atom, and the energy dependence of the transition rate for the Ni K-edge is more diffuse. The broad first maximum (if we neglect the fine structure at $\Gamma = -0.02$ au) may correspond to the scattering of the group of shells from 2.12 Å to 2.70 Å, and the flat high-energy region may correspond to the more complex photoelectron processes. The shape of the Ni K-edge transition rate is less affected by amorphization. These results are in qualitative agreement with experiment [26], although direct quantitative correlation with these data for the low-energy region is unlikely. It is interesting to test it precisely, especially for B K-edge in a-Ni₆₆B₃₄.

It is worth noting that in the present calculations no allowance has been made for the energy-dependent inverse electron lifetimes, Γ , shake-up and shake-off processes, and thermal disorder were ignored. This may set up hardly resolved problems in analysis of the contribution of the various paths, because $A^n(k, p_i)$ in (14) will include the badly defined factor $\exp(-\Gamma(E)R_i)$ and in (13) we obtain the sum of such terms.

4. Conclusion

The local order can change noticeably in some metal-metalloid systems, like Ni₂B, under amorphization. There may appear direct contact of metalloid atoms as a result of the conflict in spatial positions of small and large atoms (called here the 'packing frustration'). This effect is reproduced in a Monte Carlo simulation with a simple model for inter-atomic interactions. Because the local environment in TM–M glasses seems to be solely dictated by geometrical considerations [15], we can anticipate the similar behaviour in other analogous systems. For the ratio of constituents (TM:M) equal to 80:20 and 66:34 we find the icosahedral motifs in local coordination of the metal pairs. The calculated XAFS spectra reflect the changes in atomic structure, hence the precise measurements of K-edge absorption (especially for B atoms) in the region below 50 eV. This provides more insight into the problem of local order in glassy metals, because XAFS spectra are sensitive to the atomic coordination on the short and medium scale. From these experiments we, perhaps, can also estimate the value of photoelectron energy losses.

Acknowledgments

We appreciate valuable discussions with S T Belyaev, S N Ishmaev, S L Isakov, E Shvab and the numerical assistance of I S Tupitsyn. We are also indebted to D D Vvedensky for conversations about the XANES code [24] and to R F de Dombal for his help.

References

- [1] Sachdev S and Nelson D R 1985 *Phys. Rev. B* **32** 4592
- [2] Yonezawa F, Nose S and Sakamoto S 1988 *Z. Phys. Chem. NF* **156** 77
- [3] Gaskell P H 1983 *Glassy Metals II* ed H Beck and H-J Guntherodt (Berlin: Springer) p 12
- [4] Suzuki K, Fukunaga T, Itoh F and Watanabe N 1984 *Proc. 5th Int. Conf. Rapid Quenched Metals (Wurzburg)* Vol I, p 479
- [5] Ishmaev S N, Isakov S L, Sadikov I P, Svab E, Koszegi, Lovas A and Meszaros Gy 1987 *J. Non-Cryst. Solids* **94** 11
- [6] Bratkovsky A M and Smirnov A V 1990 *J. Non-Cryst. Solids* **117/118** 211
- [7] Bratkovsky A M and Smirnov A V 1990 *Phys. Lett* **146A** 522
- [8] Steinhardt P J, Nelson D R and Ronchetti M 1983 *Phys. Rev. B* **28** 784
- [9] Greaves G N, Durham P J, Diakun G and Quinn P 1981 *Nature* **294** 139
- [10] Gaskell P H, Glover D M, Livesey A K, Durham P J and Greaves G N 1982 *J. Phys. C: Solid State Phys.* **15** L597
- [11] Kizler P Lamparter P and Steeb S 1988 *Mat. Sci. Eng.* **97** 169
- [12] Welch D O, Dienes G J and Paskin A 1978 *J. Phys. Chem. Solids* **39** 589
- [13] Harris R and Lewis L J 1983 *J. Phys. F: Met. Phys.* **13** 1359
- [14] Fujiwara T 1984 *J. Non-Cryst. Solids* **61 + 62** 1039
- [15] Harris R and Lewis L J 1982 *Phys. Rev. B* **25** 4997
- [16] Car R and Parrinello M 1985 *Phys. Rev. Lett.* **55** 2471
- [17] Hohl D, Jones R O, Car R and Parrinello M 1988 *J. Chem. Phys.* **89** 6823
- [18] Fujiwara T, Chen H S and Waseda Y 1981 *J. Phys. F: Met. Phys.* **11** 1327
- [19] Warren B E 1969 *X-Ray Diffraction* (Reading, MA: Addison-Wesley)
- [20] Gargill G S III and Spaepen F 1981 *J. Non-Cryst. Solids* **43** 91
- [21] Andersen O K 1975 *Phys. Rev. B* **12** 3060
- [22] Durham P J, Pendry J B and Hodges C H 1981 *Solid State Commun.* **38** 159
- [23] Durham P J, Pendry J B and Hodges C H 1981 *Comput. Phys. Commun.* **25** 193
- [24] Vvedensky D D, Saldin D K and Pendry J B 1986 *Comput. Phys. Commun.* **40** 421
- [25] Brouder C, Ruiz Lopez M F, Pettifer R F, Benfatto M and Natoli C R 1989 *Phys. Rev. B* **39** 1488
- [26] Wong J and Liberman H H 1984 *Phys. Rev. B* **29** 651
- [27] Polk D E 1970 *Scr. Metall.* **4** 117